applied sciences

MDPI

Communication

Broadband DOA Estimation by Exploiting DFT Extrapolation

Euiho Shin [1], Young-seek Chung [2,*], Seonkyo Kim [3], Cheolsun Park [3] and Jungsuek Oh [1]

[1] Institute of New Media and Communications, Electrical and Computer Engineering, Seoul National University, Seoul 08826, Republic of Korea
[2] Department of Electronic Convergence Engineering, Kwangwoon University, Seoul 01897, Republic of Korea
[3] Agency for Defense Development, Daejeon 34186, Republic of Korea
* Correspondence: yschung@kw.ac.kr

Abstract: This study proposes broadband direction (DOA) estimation through discrete Fourier transform (DFT) extrapolation. We used DFT extrapolation in the lower band and extended the sampled data to reduce the beam width in the spectral domain and improved the accuracy of the estimated DOA. The sampled data with a length of 12 were extrapolated to 36 by the addition of 12-element virtual arrays to 12 real arrays on both sides. The average RMSEs of the estimated DOAs were measured throughout the wide frequency band. To verify the validity of the proposed algorithm, we demonstrated that the RMSE obtained from the broadband DOA estimation for multiple signals of interest (SOIs) was reduced in the extrapolated array. It was demonstrated that the proposed algorithm can broaden the frequency band at which a fixed number of array can estimate the DOA accurately.

Keywords: DOA estimation; broadband beamformer; DFT extrapolation

Citation: Shin, E.; Chung, Y.-s.; Kim, S.; Park, C.; Oh, J. Broadband DOA Estimation by Exploiting DFT Extrapolation. *Appl. Sci.* **2023**, *13*, 660. https://doi.org/10.3390/app13010660

Academic Editors: Fangqing Wen, Wei Liu, Jin He and Veerendra Dakulagi

Received: 20 November 2022
Revised: 28 December 2022
Accepted: 29 December 2022
Published: 3 January 2023

1. Introduction

Broadband direction-of-arrival (DOA) estimation has been actively studied to detect and estimate the origin of a signal [1–9]. In the lower band, the beam width of the DOA domain is widened [10], and the resolution is lowered accordingly, making it difficult to accurately estimate the DOA. Therefore, in some cases, it may not be possible to accurately estimate with the sampled signal alone. In a previous study [7], multiple signal classification (MUSIC) was used for broadband DOA estimation, which is impractical in terms of computational complexity.

We propose discrete Fourier transform (DFT) extrapolation to estimate the DOA in a wideband, particularly in the lower bands. Previous research [11] proposed a high-resolution algorithm called DFT extrapolation to estimate the frequency of the incoming signal in the power spectrum from a limited-number dataset. By contrast, this study applies an algorithm for broadband DOA estimation.

The remainder of this paper is organized as follows. Section 2 outlines DFT extrapolation and proposes a method for applying it to broadband DOA estimation. Section 3 describes the simulation conditions and results. In Section 4, we discuss the improvements thus achieved.

2. DFT Extrapolation

2.1. Theoretical Background

DFT extrapolation is an iterative approach suitable for spectral estimation [11]. It is performed using an algorithm capable of reconstructing an extended series of information from sampled data. In this approach, Fourier transform estimation is performed via linear inversion using original data and the minimization of a cost function [12].

The following is an explanation of the aforementioned algorithm. Assume that a length-N time series $x_0,\ x_1, x_2\ \ldots,\ x_{N-1}$ is sampled. Using zero padding, N sampled series is converted into M spectral samples:

$$\mathbf{x} = \mathbf{F}\mathbf{X}, \tag{1}$$

where $\mathbf{x} \in \mathbb{R}^N$ and $\mathbf{X} \in \mathbb{C}^M$ denote the sampled information and the unknown DFT, respectively, and $N \times M$ matrix $\mathbf{F}$ has elements $F_{n,k} = (1/M)e^{i2\pi nk/N}$. To make the solution unique, the l_2 norm cost function is augmented with a selected regularizer $\Phi(\mathbf{X})$, and is minimized. The augmented cost function J($\mathbf{X}$) is expressed as follows:

$$\mathrm{J}(\mathbf{X}) = \Phi(\mathbf{X}) + \|\mathbf{x} - \mathbf{F}\mathbf{X}\|_2^2, \tag{2}$$

where $\|.\|_2^2$ stands for l_2 norm. We set the regularizer as a Cauchy distribution, which requires iteration [13–15]. The Cauchy regularizer can be expressed as follows:

$$\Phi(\mathbf{X}) = \sum_{k=0}^{M-1} \ln\left(1 + \frac{X_k X_k^*}{2\sigma_X^2}\right), \tag{3}$$

where σ_X is a parameter of the prior distribution of $p(X|\sigma_X)$. Let us assume that the data are contaminated by noise having a distribution of $N(0, \sigma_n^2)$. Equating the derivatives of the augmented cost function to zero yields

$$\mathbf{X} = \left(\lambda\mathbf{Q}^{-1} + \mathbf{F}^{\mathrm{H}}\mathbf{F}\right)^{-1}\mathbf{F}^{\mathrm{H}}\mathbf{x} = \mathbf{Q}\mathbf{F}^{H}\left(\lambda\mathbf{I}_{\mathrm{N}} + \mathbf{F}^{\mathrm{H}}\mathbf{Q}\mathbf{F}\right)^{-1}\mathbf{x} = \mathbf{Q}\mathbf{F}^{H}\mathbf{b}, \tag{4}$$

where $\lambda = \sigma_n^2/\sigma_X^2$, $\mathbf{I}_{\mathrm{N}}$ is an $N \times N$ identity matrix, $\mathbf{Q}$ is an $M \times M$ diagonal matrix with $Q_{kk} = 1 + X_k X_k^*/2\sigma_X^2$, and H is the Hermitian transpose. The algorithm starts with the DFT of $\mathbf{x}$, $\mathbf{X}^{(0)}$, which generates matrix $\mathbf{Q}^{(0)}$. We can obtain the updated DFT by computing Equations (5) and (6), as follows:

$$\mathbf{b}^{(\mu-1)} = \left(\lambda\mathbf{I}_N + \mathbf{F}^{\mathrm{H}}\mathbf{Q}^{(\mu-1)}\mathbf{F}\right)^{-1}\mathbf{x} \tag{5}$$

$$\mathbf{X}^{(\mu)} = \mathbf{Q}^{(\mu-1)}\mathbf{F}^{H}\mathbf{b}^{(\mu-1)}, \tag{6}$$

where μ is the number of iterations. The iteration process is stopped when the (27) of [11] is satisfied.

2.2. Application for Broadband DOA Estimation

There are two differences between the method proposed in [11] and the ones used in this study. The algorithm used in this study estimates the DOA using the sampled signal. In other words, the sampled signal is a spatial series, not a time series, and the spectral domain is taken as the DOA domain in this study. The problem, however, is that the number of spatial series sampled with an antenna array is extremely small compared to the length of the sampled time series; the former is at best 30, but the latter is usually of the order of 10^2. Thus, the effect of noise is more significant when the number of samples in the series becomes smaller. Additionally, if λ is too large or the tolerance is too small in the iterative process with the Cauchy regularizer, the extrapolated signal becomes zero because the sparsity increases excessively due to the excessive iteration. We addressed this difference by heuristically adjusting the hyperparameters in the algorithm.

3. Simulation Results

3.1. Simulation Conditions

An antenna array of 12 elements was designed at 3 GHz, and the uniform interval between elements was set to be half wavelength. The 12-element antenna array was

virtually extended to 36 elements using DFT extrapolation. Twelve virtual elements were added to the left and right sides of the real array. The DOA was randomly chosen, and the number of sources was three, four, or five. We assumed that the signal from the DOA was sampled under 10 dB and 20 dB SNR, where the noise followed a Gaussian distribution, which was calculated using the average of the absolute values of the sampled signal. Given that the SNR of the sampled signal can be improved with a multi-snapshot when it comes to a lower SNR [16], the simulation was performed only under the aforementioned two SNRs. The number of spectral samples M was fixed at 1024 to achieve a high resolution of the DOA estimation results from each array. The frequency band observed was from 500 MHz to 3 GHz with a step of 0.1 GHz. The hyperparameter λ and tolerance were heuristically set to 0.003 and 0.01, respectively, throughout the frequencies.

To observe the improvement of the DFT extrapolation, we compared the estimation of arrays with virtual arrays with the estimation results using the real array before the extension and the real array with the same number of elements as the virtual array: (1) a real array with 12 elements, (2) a 12-element real array extrapolated to 36 elements, and (3) a 36-elements real array. Assuming that we already know the number of DOA, the root mean square error (RMSE) value was used as a metric to evaluate the DOA estimation result, which was obtained by averaging 1000-times repeated results at each frequency [17]. If the estimated DOA number was less than the real DOA, we set the RMSE to 45°. To determine the correlation between the estimated DOA number and RMSE, we plotted the average number of peaks greater than −15 dB in the normalized pattern in the spectral domain for each frequency.

3.2. Results

Figure 1a,b represent the DOA RMSEs measured at 10 dB and 20 dB SNR, and the number of peaks in the spectral domain, respectively, when the three randomly chosen DOAs were −31, 10, and 38°. In Figure 1a, at 10 dB SNR, the RMSEs of the 36-element real array are all within 5°. At relatively high frequencies, the RMSE of the 12-element real array was similar to that of the extrapolated array. However, at lower frequencies, a difference was observed in this regard. The RMSE of the 12-element real array exceeded 5° below 1.6 GHz, with a significant increase in the lower frequencies. When the real array was extrapolated, the RMSE exceeded 5° at 1.2 GHz but did not increase rapidly, unlike that of the 12-element real array. The reason for the rapid increase in the RMSE, as in the 12-element real arrays, was found to be highly related to the number of peaks. If the number of peaks was three or less, the DOA could not be estimated, and the RMSE will increase rapidly to 45°, as described in Section 3.1. Figure 1a shows a drastic change in the RMSE values at frequencies where the estimated number of peaks is less than three. This also occurred at an SNR of 20 dB. In Figure 1b, the RMSE of the 36-element real array remains below 5° above 600 MHz, sharp changes in the RMSE are observed at 1.5 GHz for the 12-element real array, and at 0.9 GHz for the extrapolated array. This is also related to the number of peaks. This indicates that expanding the virtual array through DFT extrapolation expands the measurable frequency band.

Figure 2a,b represent the DOA RMSEs measured at 10 dB and 20 dB SNR and the number of peaks in the spectral domain, respectively, when the four randomly chosen DOA are −36, −8, 23, and 49°. These results are similar to those shown in Figure 1. In Figure 2a, the RMSE of the 36-element real array remains below 5 degrees above 700 MHz, and sharp changes in the RMSE are seen at 2.1 GHz for the 12-element real array, and at 1.1 GHz for the extrapolated array. In Figure 2b, the RMSE of the 36-element real array remains below 5 degrees above 500 MHz, and drastic changes in the RMSE are observed at 2.1 GHz for the 12-element real array, and at 1.0 GHz for the extrapolated array. It can be observed that the changes are related to the number of peaks. Figure 2 also indicates that measurable frequency band for the four DOAs was expanded by DFT extrapolation.

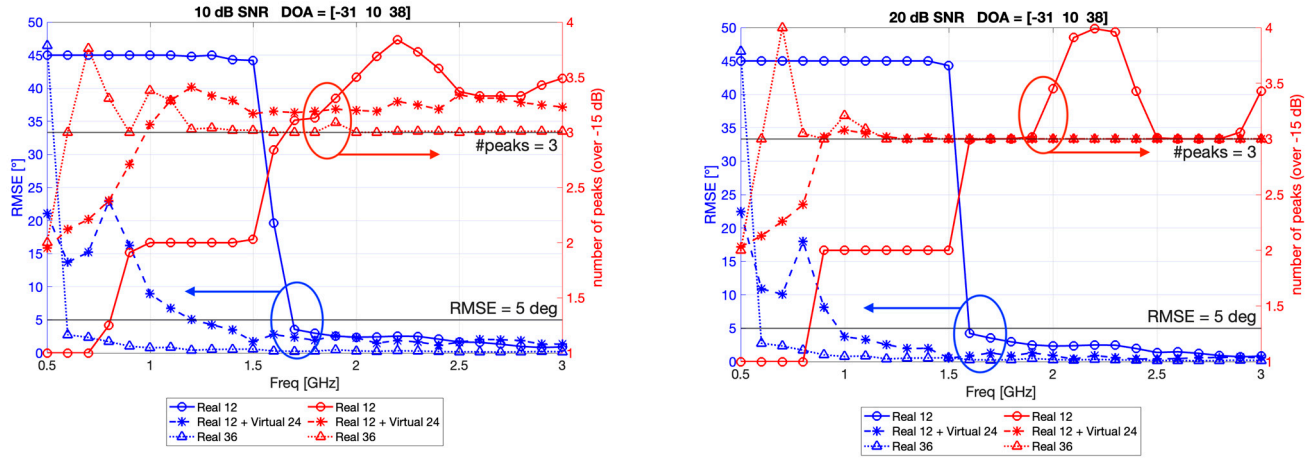

(**a**) (**b**)

Figure 1. RMSEs obtained from the DOA estimation and the number of peaks when the DOA was −31, 10, and 38° under (**a**) 10 dB SNR and (**b**) 20 dB SNR.

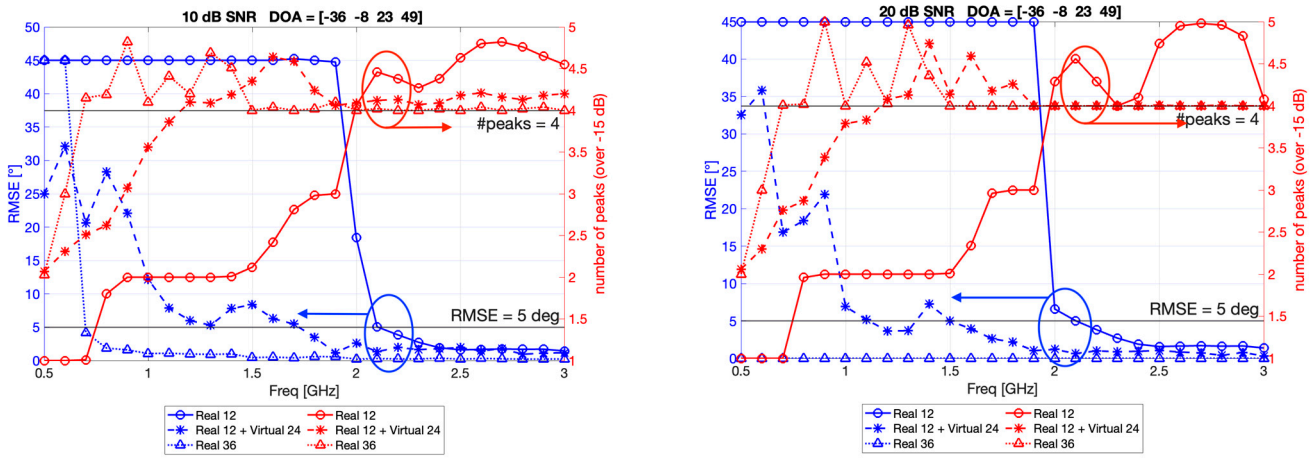

(**a**) (**b**)

Figure 2. RMSEs from the DOA estimation and the number of peaks when the DOA was −36, −8, 23, and 38° under (**a**) 10 dB SNR and (**b**) 20 dB SNR.

Figure 3a,b represent the DOA RMSEs measured at 10 dB and 20 dB SNR and the number of peaks in the spectral domain, respectively, when the five randomly chosen DOA are −68, −40, −14, 27, and 53°. In Figure 3a, the RMSE of the 36-element real array remains below 5 degrees above 1 GHz, DOAs are able to detected only at 3 GHz for the 12-element real array, and above 2.4 GHz for the extrapolated array. In Figure 3b, the RMSE of the 36-element real array remains below 5 degrees above 1 GHz, DOAs are able to be estimated only at 3 GHz for the 12-element real array, and above 1.8 GHz for the extrapolated array. Measurable frequency band for the five DOAs was expanded by DFT extrapolation as well.

The number of peaks fluctuated throughout the frequency range, even at higher frequencies. This is because the noise affects the beam patterns in the spectral domain, and peaks at an angle that is not the DOA.

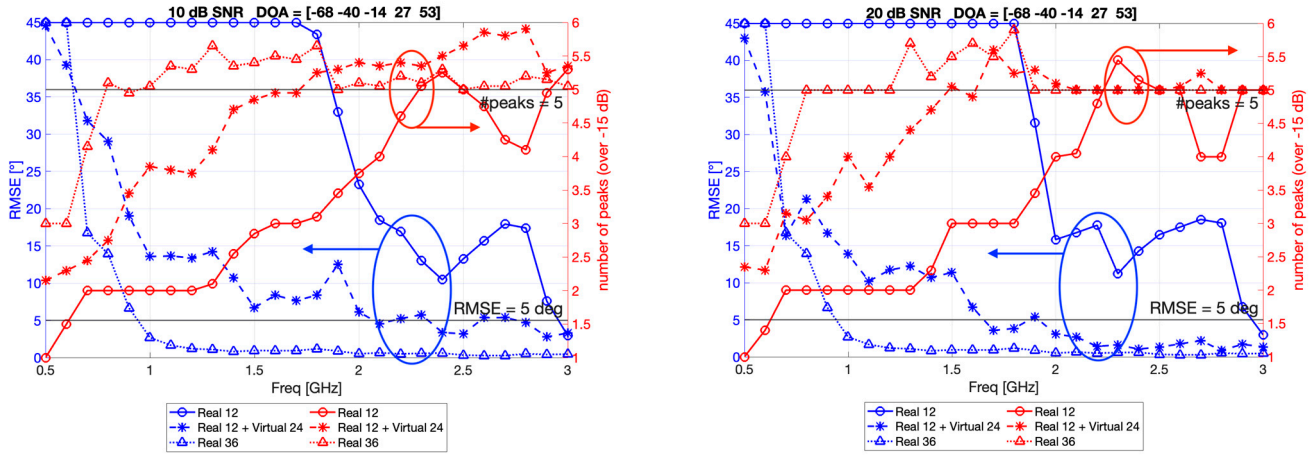

(**a**) (**b**)

Figure 3. RMSEs from the DOA estimation and the number of peaks when the DOA was −68, −40, −14, 27, and 53° under (**a**) 10 dB SNR and (**b**) 20 dB SNR.

4. Discussion

This study proposes a broadband DOA estimation method exploiting DFT extrapolation. We applied this method to the lower band to reduce the beam width in the spectral domain and improved the high-resolution property and accuracy of the estimated DOA. The received signal from randomly chosen DOAs was extended to the signal detected using the virtual 36-element array. To verify the effectiveness of the proposed algorithm, we compared the RMSEs of the DOA estimated from a 12-element array, a 12-element array extrapolated to 36-element array, and a 36-element real array at frequencies ranging from 500 MHz to 3 GHz. It was demonstrated that DFT extrapolation improved the estimation accuracy by lowering the RMSE throughout the frequency band and enabled the estimation of the DOA in the lower frequency band, which will broaden the frequency band at which an array with a relatively small number of elements can accurately estimate the DOA of a small number of sources.

Author Contributions: Conceptualization, E.S., Y.-s.C., S.K., C.P. and J.O.; methodology, E.S., Y.-s.C., S.K., C.P. and J.O.; software, E.S., Y.-s.C., S.K., C.P. and J.O.; writing—original draft preparation, E.S., Y.-s.C., S.K., C.P. and J.O.; writing—review and editing, E.S., Y.-s.C., S.K., C.P. and J.O. All authors have read and agreed to the published version of the manuscript.

Funding: This work was supported by the Agency for Defense Development by the Korean government (UD200042ED).

Institutional Review Board Statement: Not applicable.

Informed Consent Statement: Not applicable.

Data Availability Statement: Not applicable.

Conflicts of Interest: The authors declare no conflict of interest.

References

1. Shen, Z.-B.; Dong, C.-X.; Dong, Y.-Y.; Zhao, G.-Q.; Huang, L. Broadband DOA Estimation Based on Nested Arrays. *Int. J. Antennas Propag.* **2015**, *2015*, 974634. [CrossRef]
2. Ward, D.B.; Ding, Z.; Kennedy, R.A. Broadband DOA Estimation Using Frequency-Invariant Beam-Space Processing. In Proceedings of the 1996 IEEE International Conference on Acoustics, Speech, and Signal Processing Conference Proceedings, Atlanta, GA, USA, 9 May 1996; IEEE Publications: New York, NY, USA, 1996; Volume 5, pp. 2892–2895. [CrossRef]
3. Ward, D.B.; Ding, Z.; Kennedy, R.A. Broadband DOA Estimation Using Frequency Invariant Beamforming. *IEEE Trans. Signal Process.* **1998**, *46*, 1463–1469. [CrossRef]

4. Zhu, W.; Zhang, M. A Deep Learning Architecture for Broadband DOA Estimation. In Proceedings of the 19th International Conference on Communication Technology (ICCT), Xi'an, China, 16–19 October 2019; IEEE Publications: New York, NY, USA, 2019; Volume 2019, pp. 244–247. [CrossRef]
5. Chakrabarty, S.; Habets, E.A.P. Broadband DOA Estimation Using Convolutional Neural Networks Trained with Noise Signals. In Proceedings of the 2017 IEEE Workshop on Applications of Signal Processing to Audio and Acoustics (WASPAA), New Paltz, NY, USA, 15–18 October 2017; pp. 136–140. [CrossRef]
6. Mack, W.; Bharadwaj, U.; Chakrabarty, S.; Habets, E.A.P. Signal-Aware Broadband DOA Estimation Using Attention Mechanisms. In Proceedings of the ICASSP 2020—2020 IEEE International Conference on Acoustics, Speech and Signal Processing (ICASSP), Barcelona, Spain, 4–8 May 2020; IEEE Publications: New York, NY, USA, 2020; pp. 4930–4934. [CrossRef]
7. Lin, J.; Peng, Q.; Shao, H. Doubly Weighted MUSIC Algorithm for Broadband DOA Estimation Using Microphone Arrays. In *SPIE Proceedings International Conference on Space Information Technology*; SPIE: Bellingham, WA, USA, 2005; Volume 5985, pp. 472–476. [CrossRef]
8. Chen, Z.; Pei, L. A PCA-BP Fast Estimation Method for Broadband Two-Dimensional DOA of High Subsonic Flight Targets Based on the Acoustic Vector Sensor Array. In Proceedings of the 2021 14th International Congress on Image and Signal Processing, BioMedical Engineering and Informatics (CISP-BMEI), Shanghai, China, 23–25 October 2021; IEEE Publications: New York, NY, USA, 2021; pp. 1–6. [CrossRef]
9. Choo, Y.; Yang, H. Broadband Off-Grid DOA Estimation Using Block Sparse Bayesian Learning for Nonuniform Noise Variance. *IEEE J. Ocean. Eng.* **2022**, *47*, 1024–1040. [CrossRef]
10. Goodwin, M.M.; Elko, G.W. Constant Beamwidth Beamforming. In Proceedings of the IEEE International Conference on Acoustics [Speech], Minneapolis, MN, USA, 27–30 April 1993; IEEE Publications: New York, NY, USA, 1993; Volume 1, pp. 169–172. [CrossRef]
11. Sacchi, M.D.; Ulrych, T.J.; Walker, C.J. Interpolation and Extrapolation Using a High-Resolution Discrete Fourier Transform. *IEEE Trans. Signal Process.* **1998**, *46*, 31–38. [CrossRef]
12. Aboutanios, E.; Mulgrew, B. Iterative Frequency Estimation by Interpolation on Fourier Coefficients. *IEEE Trans. Signal Process.* **2005**, *53*, 1237–1242. [CrossRef]
13. Sacchi, M.D.; Ulrych, T.J. High-Resolution Velocity Gathers and Offset Space Reconstruction. *Geophysics* **1995**, *60*, 1169–1177. [CrossRef]
14. Ayeni, G.; Biondi, B. Target-Oriented Joint Least-Squares Migration/Inversion of Time-Lapse Seismic Data Sets. *Geophysics* **2010**, *75*, R61–R73. [CrossRef]
15. Tang, Y. *Target-Oriented Least-Squares Migration/Inversion with Sparseness Constraints*; Stanford Exploration Project; Stanford University, Department of Geophysics: Stanford, CA, USA, 2009; p. 171.
16. Gerstoft, P.; Mecklenbräuker, C.F.; Xenaki, A.; Nannuru, S. Multisnapshot Sparse Bayesian Learning for DOA. *IEEE Signal Process. Lett.* **2016**, *23*, 1469–1473. [CrossRef]
17. Wang, B.; Wang, W.; Gu, Y.; Lei, S. Underdetermined DOA Estimation of Quasi-Stationary Signals Using a Partly-Calibrated Array. *Sensors* **2017**, *17*, 702. [CrossRef] [PubMed]